

DTP/95/96  
CBPF-NF-079/95

RAL-TR-95-065

November 1995  
revised February 1996

# Diffractive $J/\psi$ photoproduction as a probe of the gluon density

M. G. Ryskin<sup>a</sup>, R. G. Roberts<sup>b</sup>, A. D. Martin<sup>c</sup> and E. M. Levin<sup>a,d</sup>,

<sup>a</sup> Petersburg Nuclear Physics Institute, 188350, Gatchina, St. Petersburg, Russia.

<sup>b</sup> Rutherford Appleton Laboratory, Chilton, OX11 0QX, UK.

<sup>c</sup> Department of Physics, University of Durham, Durham, DH1 3LE, UK.

<sup>d</sup> LAFEX, Centro Brasileiro de Pesquisas Fisicas, 22290-180, Rio de Janeiro, Brazil.

## Abstract

We use perturbative QCD, beyond the leading  $\ln Q^2$  approximation, to show how measurements of diffractive  $J/\psi$  production at HERA can provide a sensitive probe of the gluon density of the proton at small values of Bjorken  $x$ . We estimate both the effect of the relativistic motion of the  $c$  and  $\bar{c}$  within the  $J/\psi$  and of the rescattering of the  $c\bar{c}$  quark pair on the proton. We find that the available data for diffractive  $J/\psi$  photoproduction can discriminate between the gluon distributions of the most recent sets of partons.

## 1. Introduction

The observation of high energy diffractive  $J/\psi$  photo- or electroproduction,  $\gamma^{(*)}p \rightarrow J/\psi p$ , offers a unique opportunity to measure the gluon density in the proton at low  $x$ . Indeed, for sufficiently high  $\gamma p$  centre-of-mass energy  $W$ , perturbative QCD can be used to express the cross section for this, essentially elastic<sup>1</sup>, process in terms of the *square* of the gluon density. To lowest order the  $\gamma^* p \rightarrow J/\psi p$  amplitude can be factored into the product of the  $\gamma \rightarrow c\bar{c}$  transition, the scattering of the  $c\bar{c}$  system on the proton via (colourless) two-gluon exchange, and finally the formation of the  $J/\psi$  from the outgoing  $c\bar{c}$  pair. The crucial observation is that at high  $W$  the scattering on the proton occurs over a much shorter timescale than the  $\gamma \rightarrow c\bar{c}$  fluctuation or the  $J/\psi$  formation times, see Fig. 1.

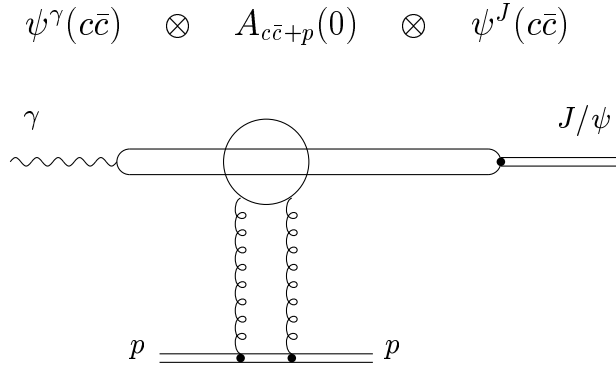


Figure 1: Schematic diagram for high energy diffractive  $J/\psi$  photoproduction. The factorized form follows since, in the proton rest frame, the formation time  $\tau_f \simeq 2E_\gamma/(Q^2 + M_\psi^2)$  is much greater than the interaction time  $\tau_{\text{int}} \simeq R$  where  $R$  is the radius of the proton.

Moreover this two-gluon exchange amplitude can be shown to be directly proportional to the gluon density  $xg(x, \overline{Q}^2)$  with

$$\overline{Q}^2 = (Q^2 + M_\psi^2)/4, \quad x = 4\overline{Q}^2/W^2. \quad (1)$$

$Q^2$  is the virtuality of the photon and  $M_\psi$  is the rest mass of the  $J/\psi$ . To be explicit, the lowest-order formula is[1]

$$\left. \frac{d\sigma}{dt} (\gamma^* p \rightarrow \psi p) \right|_0 = \frac{\Gamma_{ee} M_\psi^3 \pi^3}{48\alpha} \frac{\alpha_S(\overline{Q}^2)^2}{\overline{Q}^8} [xg(x, \overline{Q}^2)]^2 \left( 1 + \frac{Q^2}{M_\psi^2} \right). \quad (2)$$

The derivation of the result is sketched in section 2(a). An analogous formula to (2) was presented by Brodsky et al. [2] but only for longitudinally polarized vector mesons<sup>2</sup>. An earlier

<sup>1</sup>Elastic in the sense that the photon and  $J/\psi$  have the same quantum numbers.

<sup>2</sup>It has been pointed out [3] that a factor of 4 should be included in the numerator of the formula in ref. [2]. Then the results of refs. [1] and [2] agree.

work [4] presented a “soft” Pomeron treatment of diffractive vector meson production, but in this case the connection to the gluon distribution  $g(x, \overline{Q}^2)$  was not made. Here we note that the heavy meson mass  $M_\psi$  should ensure that perturbative QCD can be applied even in the photoproduction limit,  $Q^2 = 0$ . The last term in (2) allows for electroproduction via longitudinally polarised virtual photons with  $\sigma_L/\sigma_T \approx Q^2/M_\psi^2$ . The result (2) assumes a non-relativistic wave function for the  $J/\psi$  with the  $c$  and  $\bar{c}$  having momenta  $\frac{1}{2}q^J$ . Eq. (2) is derived assuming the leading  $\ln \overline{Q}^2$  approximation in the integral  $d^4k$  over the gluon loop in Fig. 1. When, in section 2, we improve on this approximation we find from the explicit form of the integral that typically  $k_T^2 \sim \overline{Q}^2$ . It is this which specifies the scale of  $\alpha_S$  in (2).

We may use the available measurements of the  $\gamma p \rightarrow J/\psi p$  production cross section (together with the observed  $J/\psi$  diffractive slope  $b = 4.5 \text{ GeV}^{-2}$ ) to give a first estimate of the gluon density. The results are shown in Fig. 2.

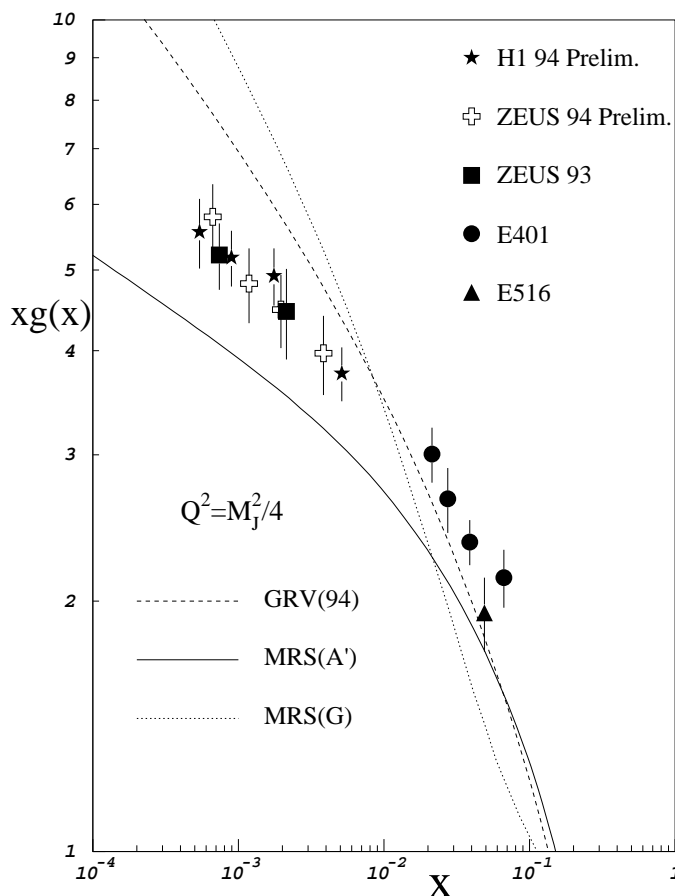


Figure 2: The points show the lowest-order estimate of the gluon density obtained from the available high energy  $\sigma(\gamma p \rightarrow J/\psi p)$  data [5,6] using eq. (2). For comparison we also show the gluon of the GRV parton set [7], and of the MRS(A', G) partons of ref.[8] evolved back to  $Q^2 = 2.5 \text{ GeV}^2$ .

This figure is simply to illustrate the typical precision and the kinematic range of the gluon density that is probed by the  $J/\psi$  data. We emphasize that it is a first look at the gluon and that the errors reflect only those of experiment. The curves correspond to gluons obtained from the latest sets of parton distributions. The spread of the predictions demonstrates the potential value of this process as a measure of the gluon. We will show that a comparison of the *shape* of the curves with the data is more reliable than that of the *normalisation*. Thus, at this preliminary stage, we see that the shape of the  $J/\psi$  data favour the MRS(A') gluon. The purpose of this paper is to refine the theory so that a meaningful probe of the gluon distribution can be obtained. However, it is already clear that diffractive  $J/\psi$  production at HERA will offer a unique, precise probe of the gluon,  $xg(x, \overline{Q}^2)$ , in the critical low  $x$ ,  $\overline{Q}^2 \gtrsim 2.5 \text{ GeV}^2$  region, *provided* that we can improve on the validity of (2).

In section 2 we scrutinise the approximations used to derive (2) and, more important, we implement corrections so that quantitative information on the gluon density can be obtained. Then, in section 3, we illustrate the discriminatory power of the diffractive  $J/\psi$  production data by comparing with the predictions of the cross section obtained from the gluon densities of the latest parton sets.

The gluon density at low  $x$  has so far been constrained by the slope of the deep inelastic structure function  $\partial F_2 / \partial \ln Q^2$ . We find that  $J/\psi$  photoproduction is a much more sensitive measure. This is only to be expected since the  $J/\psi$  photoproduction cross section depends quadratically on the gluon ( $\sigma \sim g^2$ ), whereas in deep inelastic scattering we have a linear dependence and then only on the derivative of a cross section ( $d\sigma \sim g$ ).

## 2. Improved formula for diffractive $J/\psi$ production

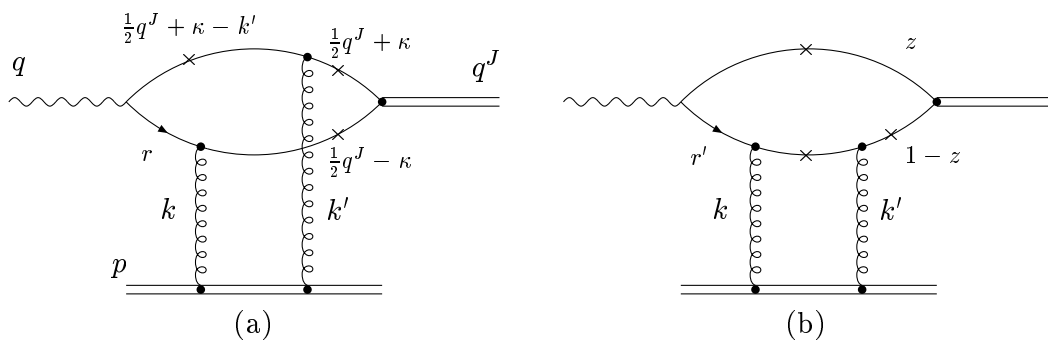


Figure 3: Lowest-order perturbative QCD diagrams for diffractive  $J/\psi$  production. The particle four-momenta are shown;  $z$  and  $1-z$  denote the fractions of the longitudinal momentum of the photon that are carried by the  $c, \bar{c}$  quarks. The small crosses indicate which quarks may be regarded as essentially on-mass-shell.

The amplitude for  $\gamma^{(*)}p \rightarrow J/\psi p$  is obtained, in lowest-order perturbative QCD, from the sum of the two diagrams shown in Fig. 3. Formula (2) is based on the leading  $\ln Q^2$

approximation in which we assume that the gluon transverse momenta  $k_T$  satisfies  $k_T^2 \ll \overline{Q}^2$ . Moreover the non-relativistic form is taken for the  $J/\psi$  wave function

$$\psi^J(z, \kappa_T) = \delta^{(2)}(\kappa_T) \delta\left(z - \frac{1}{2}\right) \quad (3)$$

where  $z = \frac{1}{2} + \kappa_{\parallel}/q_{\parallel}^{\gamma}$ . In other words, the  $c$  and  $\bar{c}$  quarks are not allowed to have any Fermi momentum inside the  $J/\psi$ , i.e.  $\vec{\kappa}$  is set to zero. We discuss these, and other, approximations in turn below. In particular we compute the corrections which should be applied before confronting (2) with the data.

### (a) Beyond the leading $\ln Q^2$ approximation; inclusion of the gluon $k_T$

Since we are primarily concerned with diffractive  $J/\psi$  photoproduction at small  $x$  we work in the (leading order)  $\ln 1/x$  approximation, and retain the full  $Q^2$  dependence and not just the leading  $\ln Q^2$  component. We must therefore express the cross section in terms of an integral over the (square of the) unintegrated gluon distribution  $f(x, k_T^2)$ , and so retain the explicit gluon  $k_T$  dependence.

We first evaluate the gluon loops in the Feynman diagrams shown in Fig. 3. It is convenient to perform the loop integrations in terms of Sudakov variables. That is the various particle four momenta are decomposed in the form

$$k_i = \alpha_i q' + \beta_i p' + \vec{k}_{iT} \quad (4)$$

where  $p'$  and  $q'$  are the proton and photon light-like momenta:  $p'^2 = q'^2 = 0$  and  $W^2 = 2p' \cdot q'$ . In particular

$$p = p' + \alpha_p q', \quad q = q' + \beta_\gamma p' \quad (5)$$

with  $\alpha_p = m_p^2/W^2$  and  $\beta_\gamma = -Q^2/W^2$ . Within the non-relativistic approximation the quarks of momenta  $\frac{1}{2}q^J \pm \kappa$  are almost on-mass-shell.

The integration over the gluon longitudinal momentum puts, in the first diagram, the upper quark with momentum  $h = \frac{1}{2}q^J + \kappa - k'$  on-shell, leaving only the quark propagator  $(r^2 - m_c^2)^{-1}$  to be integrated over in the gluon  $k_T$  integration. To express the propagator in terms of  $k_T^2$  we first note that

$$r^2 = (q - h)^2 = q^2 - 2q \cdot h + m_c^2. \quad (6)$$

Using the Sudakov decomposition

$$h = \alpha_h q' + \beta_h p' - k'_T \quad (7)$$

we obtain

$$2q \cdot h = (\beta_\gamma \alpha_h + \beta_h) W^2 = -z Q^2 + (m_c^2 + k_T'^2)/z, \quad (8)$$

where we have neglected  $\kappa_T$ . Moreover in the non-relativistic approximation  $z = \frac{1}{2}$  and so from (6) and (8) we find

$$r^2 - m_c^2 = -2\overline{Q}^2 - 2k_T^2 \quad (9)$$

where  $\overline{Q}^2 = (Q^2 + M_\psi^2)/4$ , with  $Q^2 = -q^2$ , as usual. Here we take  $M_\psi^2 \simeq 4m_c^2$ . In Fig. 3(b) only the quark with momentum  $r'$  is off-shell. In analogy to the derivation of (9) we find

$$r'^2 - m_c^2 = -2\overline{Q}^2.$$

Thus the forward scattering amplitude for diffractive  $J/\psi$  production from transversely polarized photon is

$$A = i 4\pi^2 M_\psi \alpha_S \int \frac{dk_T^2}{k_T^4} \left( \frac{1}{2\overline{Q}^2} - \frac{1}{2\overline{Q}^2 + 2k_T^2} \right) G(k) e_c g_J \quad (10)$$

where colour factors give rise to the opposite sign of the two diagrams, and where the amplitude is defined by

$$\frac{d\sigma}{dt} (\gamma_T p \rightarrow J/\psi p) = \frac{|A|^2}{16\pi}.$$

The constant  $g_J$  specifies the  $c\bar{c}$  coupling to the  $J/\psi$  and  $e_c$  is the charge of the  $c$  quark. The coupling  $g_J$  may be determined from the width  $\Gamma_{ee}$  of the  $J/\psi \rightarrow e^+e^-$  decay, a process which is described by the same  $c\bar{c}$  quark loop structure. We have

$$e_c^2 g_J^2 = \frac{\Gamma_{ee} M_\psi}{12\alpha}$$

where  $e_c^2 = \frac{4}{9} 4\pi\alpha$ . The function  $G(k)$  specifies the probability of finding the gluons in the proton. In the simplest three valence quark model

$$G = \frac{4}{3} \frac{\alpha_S}{\pi} 3 \quad (11)$$

where  $\frac{4}{3}$  is the colour factor.

In the realistic case

$$G(k) = f_{\text{BFKL}}(x, k_T^2) \quad (12)$$

where  $f_{\text{BFKL}}$  is the gluon density unintegrated over  $k_T$  that satisfies the BFKL equation, an equation which effectively resums the leading  $\alpha_S \ln(1/x)$  contributions. To gain insight into this identification, and to specify the value of  $x$ , it is sufficient to study the one-rung contribution sketched in Fig. 4.

To determine the momentum fractions  $x$  and  $x'$  of the gluons in Fig. 4 we note that

$$x + x' = \beta_\psi - \beta_\gamma = \frac{Q^2 + M_\psi^2}{W^2} \quad (13)$$

$$x' = \beta_{\text{out}} - \beta_{\text{in}} = \frac{k_T^2}{W^2 z} \quad (14)$$

where the  $\beta_i$  are the fractions of the  $p'$  momentum carried by the various particles  $i$  (see (4)) and where for simplicity we neglect  $\kappa_T$  in the quark loop.

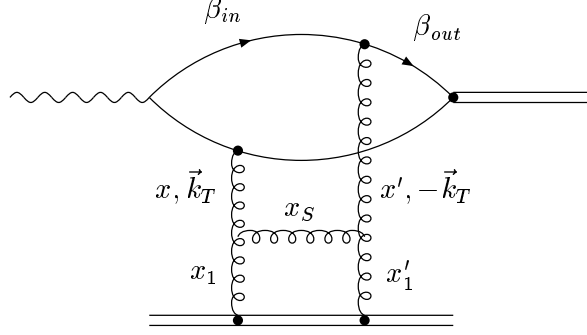


Figure 4: One of the one-rung diagrams which give the  $\alpha_S \ln(1/x)$  contribution to the BFKL gluon,  $f_{\text{BFKL}}(x, k_T^2)$ . The emitted gluons have proton momentum fractions  $x$  and  $x'$  with  $|x'| \ll x$ .

Thus, we see that  $|x'| \ll x$ . The entire<sup>3</sup> origin of the  $x$  dependence of Fig. 4 comes from the integral over the rapidity of the  $s$ -channel gluon

$$\int_x^1 \frac{dx_s}{x_s} \quad (15)$$

where the limit<sup>4</sup> comes from  $x_s = x_1 - x \simeq x_1 > x$ . This is the origin of the BFKL  $\ln(1/x)$  contribution<sup>5</sup>. Diagrams with further gluon rungs give  $\alpha_S^n \ln^n(1/x)$  contributions which are all resummed by the BFKL equation for unintegrated gluon density  $f_{\text{BFKL}}(x, k_T^2)$ , with

$$x \approx (Q^2 + M_\psi^2)/W^2 = 4\bar{Q}^2/W^2.$$

To relate  $f_{\text{BFKL}}$  to the conventional gluon density, which satisfies GLAP evolution, we must integrate over  $k_T^2$

$$xg(x, Q^2) = \int^{Q^2} \frac{dk_T^2}{k_T^2} f_{\text{BFKL}}(x, k_T^2), \quad (16)$$

and so the  $\gamma_T^{(*)} p \rightarrow J/\psi p$  forward amplitude (10) becomes

$$A = i4\pi^2 M_\psi e_{cJ} \alpha_S \int_0^\infty \frac{dk_T^2}{2\bar{Q}^2(\bar{Q}^2 + k_T^2)} \frac{\partial(xg(x, k_T^2))}{\partial k_T^2}. \quad (17)$$

The integral converges for  $k_T^2 \gg \bar{Q}^2$ , but the gluon distribution  $xg(x, k_T^2)$  is not known as  $k_T^2 \rightarrow 0$ . We therefore write

$$A \simeq i2\pi^2 M_\psi e_{cJ} \alpha_S \left[ \frac{xg(x, Q_0^2)}{\bar{Q}^4} + \int_{Q_0^2}^\infty \frac{dk_T^2}{\bar{Q}^2(\bar{Q}^2 + k_T^2)} \frac{\partial xg(x, k_T^2)}{\partial k_T^2} \right], \quad (18)$$

<sup>3</sup>Recall that spin-one  $t$  channel gluon exchange leads to an energy independent (that is  $x$  independent) cross section.

<sup>4</sup>In general the limit is  $x_s > \max\{x, x'\}$ , but in our case  $x \gg |x'|$ .

<sup>5</sup>The virtual diagrams which lead to the Reggeisation of the  $t$  channel gluons also have the same  $\ln(1/x)$  structure.

where in the first term in the brackets we have neglected the effects of  $k_T^2$  in comparison with  $\overline{Q}^2$ . Eq. (18) allows the effects of the gluon  $k_T$  to be estimated. Eq. (18) is true to  $\mathcal{O}(Q_0^2/\overline{Q}^2)$ ; we investigate below the sensitivity of our results to variation of the choice of  $Q_0^2$ . The modification of (2) becomes apparent when we use (18) to calculate the forward production cross section. We have

$$\left. \frac{d\sigma}{dt} (\gamma^* p \rightarrow \psi p) \right|_0 = \frac{\Gamma_{ee} M_\psi^3 \pi^3}{48\alpha} \alpha_S(\overline{Q}^2)^2 \left[ \dots \right]^2 \left( 1 + \frac{Q^2}{M_\psi^2} \right), \quad (19)$$

where the [...] contain the entry shown in brackets in (18). In fact the accuracy of formula (19) is even better than the BFKL approximation since the main part of the corrections may be hidden inside the experimentally determined values of  $g(x, Q^2)$  and  $\Gamma_{ee}$ . To be more precise, if we neglect the  $t_{\min}$  effects of section 2(b), eq. (17) is valid for a gluon distribution obtained from any evolution equation.

### (b) Discussion of $t_{\min}$ effects

We have tacitly assumed that we are considering a forward “elastic” scattering amplitude with  $t = 0$ . However, for  $\gamma p \rightarrow J/\psi p$  the minimum value of  $|t|$  is

$$t_{\min} = \left( \frac{Q^2 + M_\psi^2}{W^2} m_p \right)^2 \simeq x^2 m_p^2. \quad (20)$$

This result is evident from (13); we have to transfer longitudinal momentum through the  $t$ -channel two-gluon exchange. We have already checked that the difference between the momentum fractions  $x$  and  $x'$  of the two gluons does not affect the BFKL identification (12) of  $G$ ; it contributes beyond the leading  $\ln(1/x)$  approximation. For GLAP we could, in principle, recalculate Fig. 4 with Altarelli-Parisi kernels [9] which take into account the difference  $x \neq x'$ . Alternatively we can estimate the effect from the analytic structure of  $A$  in the complex  $t$  plane, where the nearest singularity is the  $2\pi$  threshold at  $t_0 = 4m_\pi^2$ . Extrapolation from  $t_{\min}$  to  $t = 0$ , where the identification  $xg(x, \overline{Q}^2)$  is true, gives at most a correction of order  $t_{\min}/t_0$ . In fact the  $2\pi$  singularity is weak, and  $t_0 \sim m_\rho^2$  is a more representative value [10]. In any case we expect the  $t_{\min}$  effects to be small for  $x < 0.1$ .

### (c) Relativistic effects in the $J/\psi$ wave function

Here we discuss the effect of the motion of the quarks within the  $J/\psi$ . This Fermi motion has been considered in ref. [11] where it was concluded that it will lead to a significant suppression of the cross section for diffractive production. Only longitudinal vector meson production was studied there, whereas for photoproduction we have to deal with transversely polarised  $J/\psi$  mesons.



To estimate these relativistic effects we combine knowledge of the  $J/\psi$  wave function  $\psi^J(\kappa_T, z)$  with the structure of the coupling of the photon to the  $c\bar{c}$  pair. For transverse and longitudinally polarised photons the amplitudes are of the form <sup>6,7</sup>

$$A(\gamma^T p \rightarrow J/\psi p) \propto \frac{1}{m_c} \int \frac{2[z^2 + (1-z)^2]\kappa_T^2 \tilde{Q}^2 + m_c^2(\tilde{Q}^2 - \kappa_T^2)}{(\tilde{Q}^2 + \kappa_T^2)^3} xg(x, \tilde{Q}^2 + \kappa_T^2) \psi^J(\kappa_T, z) \times d^2\kappa_T dz \quad (21)$$

$$A(\gamma^L p \rightarrow J/\psi p) \propto \int \frac{2z(1-z)\sqrt{Q^2}(\tilde{Q}^2 - \kappa_T^2)}{(\tilde{Q}^2 + \kappa_T^2)^3} xg(x, \tilde{Q}^2 + \kappa_T^2) \psi^J(\kappa_T, z) d^2\kappa_T dz \quad (22)$$

where  $\tilde{Q}^2 = z(1-z)Q^2 + m_c^2$  and  $x = (Q^2 + M_\psi^2)/W^2$ . These expressions may be compared with the simplified non-relativistic approximation in which we take  $z = \frac{1}{2}$  and  $\kappa_T = 0$ , see (3). Thus, if we have knowledge of the  $J/\psi$  wave function we can compute the correction factor  $F^2$  arising from the use of a more realistic  $J/\psi$  wave function. In particular, for  $J/\psi$  photoproduction we have from (21)

$$F^2 = \left| \frac{\int (1 + v_T^2)^{-3} xg(x, m_c^2(1 + v_T^2)) \psi^J(\kappa_T, z) dv_T^2}{xg(x, m_c^2) \int \psi^J(\kappa_T, z) dv_T^2} \right|^2 \quad (23)$$

with  $v_T^2 = \frac{2}{3}v^2 = \kappa_T^2/m_c^2$  where  $v$  is the velocity of the quarks in the  $J/\psi$  rest frame. In writing (23) we have set  $z = \frac{1}{2}$  in the numerator, consistent with the approximation of neglecting contributions of  $\mathcal{O}(v_T^4)$ .

If we take a Gaussian form for the  $J/\psi$  wave function,  $\psi^J = A \exp(-a \kappa_T^2/m_c^2)$ , then  $\langle v_T^2 \rangle = \frac{2}{3}\langle v^2 \rangle = 1/2a$ . Estimates of  $\langle v^2 \rangle$  obtained from studies of charmonium [13] vary in the range  $0.12 \lesssim \langle v^2 \rangle \lesssim 0.25$ , with for example a recent lattice calculation [14] giving  $\langle v^2 \rangle$  values in the interval 0.18 to 0.12 as  $m_c$  increases from 1.45 to 1.85 GeV. If we evaluate (23) using these ranges of  $\langle v^2 \rangle$  and  $m_c$  for each of the three recent sets of partons [GRV, MRS(A', G)] then we find that the suppression  $F^2$  of the cross section for diffractive  $J/\psi$  photoproduction at HERA lies in the interval

$$0.4 \lesssim F^2 \lesssim 0.6. \quad (24)$$

The suppression due to the factor  $(1 + v_T^2)^{-3}$  is partly compensated by the larger scale at which the gluon is evaluated. An independent study of the relativistic corrections to  $J/\psi$  photoproduction has been made by Jung et al. [15]. Using the gluonic and leptonic widths of

---

<sup>6</sup>Here we neglect  $k_T$  in comparison with  $\kappa_T$ . It is straightforward to derive formulae in the presence of both  $k_T$  and  $\kappa_T$ . To simplify the presentation we choose to investigate these corrections in turn and hence impose the leading  $\log Q^2$  approximation in eqs. (21) and (22) [1,2]. Correlated effects will occur, but at the level of other uncertainties.

<sup>7</sup>Eqs. (21) and (22) are derived assuming the form of the  $J/\psi$  light cone wave function given in (2.22) of ref. [2]. The derivation is subtle and will be presented elsewhere in a more general study of diffractive vector meson production[12].

the  $J/\psi$  they estimate  $\langle v^2 \rangle = 0.16$  with  $m_c = 1.43$  GeV, values which are quite compatible with the above estimates. The correction factor  $F^2$  evaluated using these values of  $\langle v^2 \rangle$  and  $m_c$  is shown in Table 1 over the range of  $x$  relevant to diffractive  $J/\psi$  photoproduction at HERA.

Table 1: The correction factor  $F^2$  of (23) evaluated using three recent sets of partons.

| $x$                | $F^2$ (GRV) | $F^2$ (A') | $F^2$ (G) |
|--------------------|-------------|------------|-----------|
| $5 \times 10^{-4}$ | 0.46        | 0.54       | 0.48      |
| $10^{-3}$          | 0.45        | 0.52       | 0.47      |
| $2 \times 10^{-3}$ | 0.45        | 0.50       | 0.47      |
| $5 \times 10^{-3}$ | 0.44        | 0.48       | 0.46      |

Besides the correction factor coming from the  $J/\psi$  wave function weighted by the  $\gamma \rightarrow c\bar{c}$  coupling, we have to consider the effect arising from the inequality  $2m_c \neq M_\psi$ . At first sight such a kinematic effect might appear to be negligible. However we note that eq. (2) is written in terms of  $M_\psi^2$ , while in eqs. (21) and (22) the current quark mass  $m_c$  enters. Thus we see that eq. (2) comes from eqs. (21) and (22), in the small  $\kappa_T$  limit, with  $m_c^2$  replaced by  $\frac{1}{4}M_\psi^2$ . The other factors, such as the leptonic width and the photon propagator, depend directly on  $M_\psi$ . So for photoproduction, with  $Q^2 = 0$ , the total relativistic correction factor is estimated to be

$$F^2 \left( \frac{M_\psi}{2m_c} \right)^8 \approx 1 \quad (25)$$

with a large uncertainty of at least  $\pm 30\%$ . Thus it turns out that the best prescription is as follows. We should replace  $m_c^2$  by  $\frac{1}{4}M_\psi^2$  in eqs. (21) and (22) so that the mass factor disappears from eq. (25) and the correction factor  $F^2$  becomes closer to 1. Of course this does not decrease the overall uncertainty. However we emphasize that the uncertainty mainly affects the normalization of the gluon density extracted from  $J/\psi$  diffractive data, and that the prediction for the  $x$  dependence should be much more reliable. We see from Table 1 that the gluon density leads to a small  $x$  dependence of  $F^2$ , which we neglect in our comparison with the data below, but which should be included when the  $J/\psi$  data become more precise.

We see from (21) and (22) that the suppression  $F^2$ , arising from the use of the relativistic wave function, decreases with increasing  $Q^2$  due to the presence of the  $z(1-z)Q^2$  term. In fact since

$$z(1-z) \approx \frac{1}{4}(1 - \langle v_z^2 \rangle), \quad (26)$$

where  $\langle v_z^2 \rangle = \frac{1}{3}\langle v^2 \rangle$ , we even expect, as  $Q^2$  increases, that eventually the factor  $F^2$  will give an enhancement, *not* a suppression, of the cross section. When we take Fermi motion into account the ratio of diffractive  $J/\psi$  production from longitudinal and transverse photons becomes

$$\frac{\sigma_L}{\sigma_T} \approx \frac{Q^2}{4m_c^2} (1 - \langle v^2 \rangle)^2. \quad (27)$$

Our result disagrees with the conclusions of ref.[11] where a large suppression (of at least a factor of 3) was found to arise from Fermi motion. There are several differences in our calculations. First ref.[11] uses a potential model  $J/\psi$  wave function whereas here we employ a Gaussian form. Our considered range of  $\langle v^2 \rangle$  embraces a large class of wave functions and covers the results obtained using the wave function of any reasonable charmonium model. (Incidentally it is worth mentioning that the recent lattice calculation[14] gives a wave function better described by a Gaussian form than by the more sophisticated potential models). However, most of the difference between our results and that of ref.[11] has a different origin. Part of the difference is due to the inclusion of the mass factor in (25). The remaining discrepancy arises from the use of the appropriate wave function of the virtual photon and the use of the correct scale for the gluon in eq. (21).

#### (d) Rescattering or absorption of $c\bar{c}$ quark-pair

The shadowing effects of the gluons are already included in  $xg(x, \bar{Q}^2)$  if the distribution is determined in a global parton analysis of experimental data. Here we are concerned with the rescattering or absorption of the  $c\bar{c}$  pair as it transverses through the proton. A typical diagram is shown in Fig. 5. Let us study the first shadowing correction (with  $n = 1$ ) arising from the exchange of one extra pair of gluons with transverse momenta  $\pm \vec{K}_T$ , where the Sudakov decomposition (see (4)) of the gluon 4-momentum is

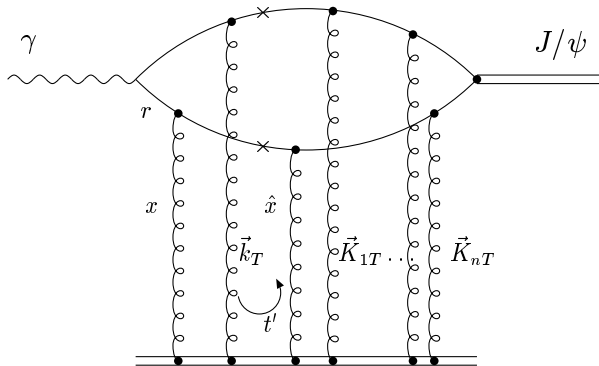


Figure 5: A typical diagram leading to a  $c\bar{c}$  rescattering correction. In the text we compute the  $n = 1$  contribution. All quark lines are on-shell except for that with momentum  $r$ , as in Fig. 3.

$$K_1 \equiv K = \alpha_K p' + \beta_K q' + \vec{K}_T. \quad (28)$$

To compute the extra gluon loop we first close the contour of the integrations over  $\alpha_K$  and  $\beta_K$  on the quark propagators marked by small crosses on Fig. 5. Hence we again have all quarks on-mass-shell, except for that with momentum  $r$ . Thus we do not change the result of the integration over the  $c\bar{c}$  loop. If we take into account the four different ways the extra gluons

can couple to the  $c$  and  $\bar{c}$ , then we have to include a total of 16 diagrams, and the integration over  $\vec{k}_T$  and  $\vec{K}_T$  gives, in analogy with (10), an amplitude of the form

$$\int \frac{d^2 k_T}{k_T^4} \int \frac{d^2 K_T}{K_T^4} \frac{1}{2} \left[ \frac{2}{\bar{Q}^2} - \frac{2}{\bar{Q}^2 + k_T^2} - \frac{2}{\bar{Q}^2 + K_T^2} + \frac{1}{\bar{Q}^2 + |\vec{k}_T + \vec{K}_T|^2} + \frac{1}{\bar{Q}^2 + |\vec{k}_T - \vec{K}_T|^2} \right] f_{\text{BFKL}}(x, k_T^2) f_{\text{BFKL}}(\hat{x}, K_T^2). \quad (29)$$

We again neglect  $\kappa_T$ . The non-zero value of  $\hat{x}$  arises because we have to put a quark on-shell with an additional momentum  $\vec{K}_T$ . We therefore need to transfer to the quark a proton momentum fraction

$$\hat{x} = \frac{K_T^2}{zW^2} \simeq \frac{\bar{Q}^2}{2zW^2} \simeq \frac{x}{4}, \quad (30)$$

since typically we have  $K_T^2 \sim \bar{Q}^2/2$ . For  $k_T, K_T \ll \bar{Q}$ , after neglecting the angular correlation between  $\vec{k}_T$  and  $\vec{K}_T$ , that is setting

$$\langle (\vec{k}_T \cdot \vec{K}_T)^2 \rangle = \frac{1}{2} k_T^2 K_T^2,$$

the expression in square brackets in (29) becomes

$$\frac{1}{2} [\dots] = \frac{k_T^2}{\bar{Q}^4} \frac{4K_T^2}{\bar{Q}^2}.$$

We expand the integrand in (29) assuming that  $k_T^2, K_T^2 \ll \bar{Q}^2$ . If we keep the leading terms then we find

$$\frac{\Omega}{2} = \frac{\pi \alpha_S(\bar{Q}^2)}{3b} \int \frac{dK_T^2}{\bar{Q}^2 + K_T^2} \frac{\partial(\hat{x}g(\hat{x}, K_T^2))}{\partial K_T^2}, \quad (31)$$

where  $\Omega$  is defined so that the correction to the amplitude is

$$A = A_0(1 - \frac{1}{2}\Omega). \quad (32)$$

As the correction is not too large we can eikonalize (31) by hand, directly in the momentum representation, and write the final expression in the form

$$\sigma = \sigma_0 \exp(-\Omega). \quad (33)$$

The factor  $1/b$  in (31) comes from the integral over the “reggeon” loop in Fig. 5

$$\int dt' e^{-bt'} = 1/b, \quad (34)$$

where we use the experimental slope  $b = 4.5 \text{ GeV}^{-2}$ . The  $K_T^2$  integration in (31) is evaluated just as in (17) and (18).

It is worthwhile mentioning that the simple estimate of (31) is in good agreement with the more detailed treatment of ref. [16].

### (e) Next-to-leading order corrections

There are expectations that higher-order radiative corrections will have a negligible effect. We refer to four possible types of radiation shown all together in Fig. 6.

The contribution of the diagram with the single extra gluon denoted by (a) is already incorporated in  $\Gamma(J/\psi \rightarrow e^+e^-)$ , while (b) is hidden in  $\alpha_S$  and (c) is subsumed in  $xg(x, Q^2)$ . Only correction (d) survives, but this is suppressed by a factor  $\tau_{\text{int}}/\tau_f$ , which is small for high  $W$ , that is for  $x \ll 1$ , see the comment in the caption to Fig. 1.

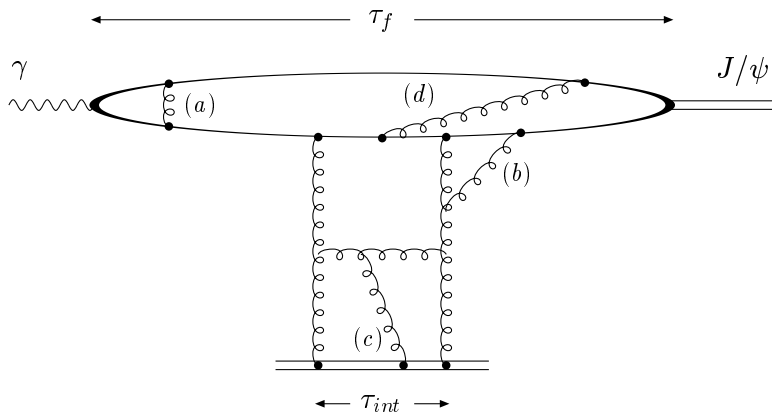


Figure 6: Four different types of radiative correction, denoted by (a,b,c,d), are shown together on the lowest-order diagram for diffractive  $J/\psi$  production.

Independent evidence for small radiative effects comes from a study of next-to-leading order corrections in *inelastic*  $J/\psi$  production at HERA [17]. The lowest-order subprocess is shown in Fig. 7. It is found that the corrections to inelastic  $J/\psi$  production are in general appreciable ( $\gtrsim 50\%$ ). However, they reduce almost to zero when  $\hat{s} \rightarrow M_\psi^2$ , that is when the emitted gluon  $k$  is very soft, which corresponds to our pomeron with  $|x'| \ll x$ , see (14).

### (f) Inclusion of the real part

So far we have calculated only the imaginary part of the amplitude. At high energy  $W$ , that is at small  $x$ , our positive-signature amplitude behaves as

$$A \propto x^{-\lambda} + (-x)^{-\lambda}.$$

Providing  $\lambda$  is small, the amplitude is dominantly imaginary and the real part can be calculated as a perturbation

$$\frac{\text{Re}A}{\text{Im}A} \approx \frac{\pi}{2}\lambda \approx \frac{\pi}{2} \frac{\partial \ln A}{\partial \ln(1/x)} \approx \frac{\pi}{2} \frac{\partial \ln(xg(x, \overline{Q}^2))}{\partial \ln(1/x)}. \quad (35)$$

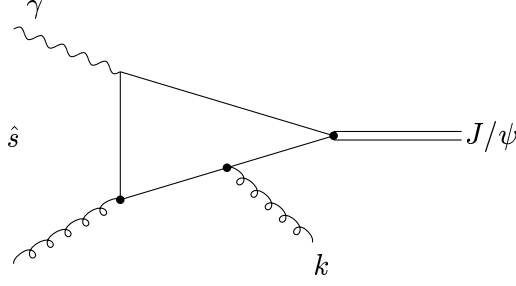


Figure 7: The lowest-order subprocess,  $\gamma g \rightarrow J/\psi g$ , describing inelastic  $J/\psi$  production. The emitted gluon  $k$  is necessary to satisfy the colour and spin constraints of the  $J/\psi$ .

### 3. Comparison with diffractive $J/\psi$ photoproduction data

We use the perturbative QCD formula (19) together with the corrections which we detailed in section 2, to calculate the cross section for diffractive  $J/\psi$  photoproduction

$$\sigma(\gamma p \rightarrow J/\psi p) = \frac{1}{b} \frac{d\sigma}{dt} (\gamma p \rightarrow J/\psi p) \Big|_0$$

as a function of the  $\gamma p$  centre-of-mass energy  $W$ . We take the experimental value for the slope parameter:  $b = 4.5 \text{ GeV}^{-2}$ . The prediction depends on the square of the gluon density,  $[xg(x, \overline{Q}^2)]^2$ , at  $x = M_\psi^2/W^2$  and for values of  $\overline{Q}^2$  in the region of  $M_\psi^2$ . For illustration we calculate the  $W$ -dependence of the cross section using the gluon distributions of three of the latest sets of partons, namely GRV [7] and MRS(A', G) [8]. The latter partons are extrapolated below  $Q^2 = 4 \text{ GeV}^2$  with next-to-leading GLAP evolution.

It could be argued that it is inappropriate to use GLAP-based gluons in our resummed  $\log(1/x)$  formalism. However, they should be regarded simply as a parametrization of the data. The non-perturbative parameters are a good representation of all physical effects such as BFKL smearing and shadowing corrections. It is well known that the present data cannot distinguish the underlying perturbative physics. However, data do distinguish between the parametrizations.

The three predictions are compared with the available high energy  $J/\psi$  photoproduction data in Fig. 8. The curves correspond to the choice of lower limit  $Q_0^2 = 1 \text{ GeV}^2$  in the integral over the gluon  $k_T^2$  in (19). We explored the sensitivity of the predictions to variation of  $Q_0^2$  over the range 0.5 to 2  $\text{GeV}^2$  for the GRV gluon, and 1 to 4  $\text{GeV}^2$  for the MRS gluons. Depending on the parton set, the cross section values change by  $\pm 15\%$  at  $W = 10 \text{ GeV}$ , increasing to  $\pm 25\%$  at  $W = 100 \text{ GeV}$  as  $Q_0^2$  is varied.

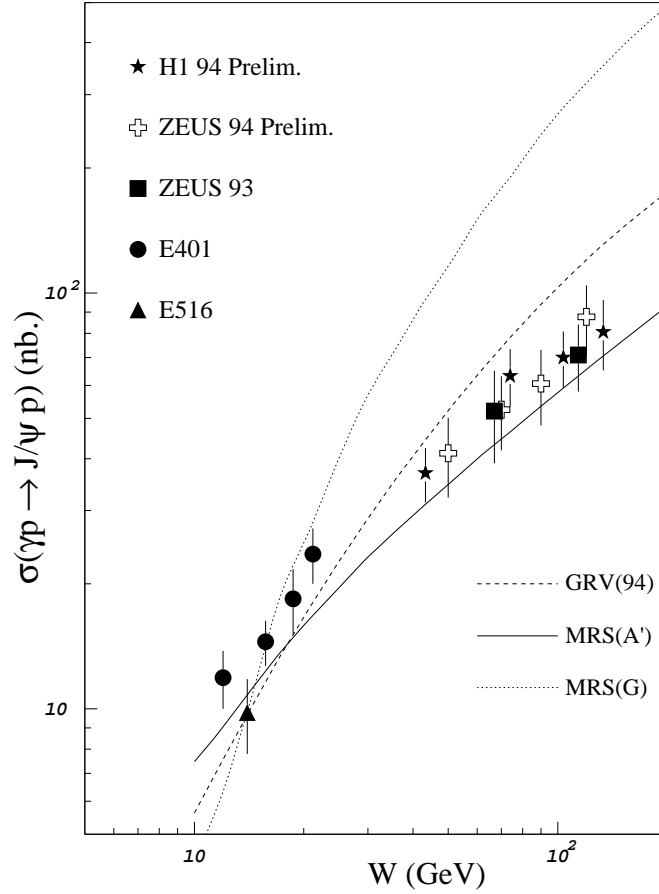


Figure 8: The measurements [5,6] of the cross section for diffractive  $J/\psi$  photoproduction compared with the full perturbative QCD prediction, as described in section 2, obtained from the three latest sets of partons.

In Table 2 we quantify the effect of sequentially improving the prediction of the lowest-order formula (2), first to (19), which goes beyond the leading  $\ln Q^2$  approximation to include the effects of the transverse momenta of the exchanged gluons, and then to include the factor  $\exp(-\Omega)$ , with  $\Omega$  given by (31), to allow for the  $c\bar{c}$  rescattering on the proton. Table 2 shows the size of the effects at  $W = 100$  GeV. We see that the two corrections to the lowest-order formula partially compensate each other. The corrections decrease with decreasing energy  $W$ , and are found to be insignificant for  $W \lesssim 20$  GeV.

Table 2: The cross section for diffractive  $J/\psi$  photoproduction

| Partons  | $\sigma(\gamma p \rightarrow J/\psi p)$ in nb at $W = 100$ GeV |                |                       |
|----------|--|----------------|-----------------------|
|          | lowest-order   | + gluons $k_T$ | + $c\bar{c}$ rescatt. |
| GRV      | 128  | 157            | 88                    |
| MRS (A') | 47   | 79             | 55                    |
| MRS (G)  | 262  | 331            | 208                   |

In addition to the above effects, the predictions shown in Fig. 8 also include the real part contribution via (35). According to (25) the  $J/\psi$  relativistic effects are estimated to leave the cross section unaltered, but to introduce a sizeable normalization uncertainty.

## 4. Conclusions

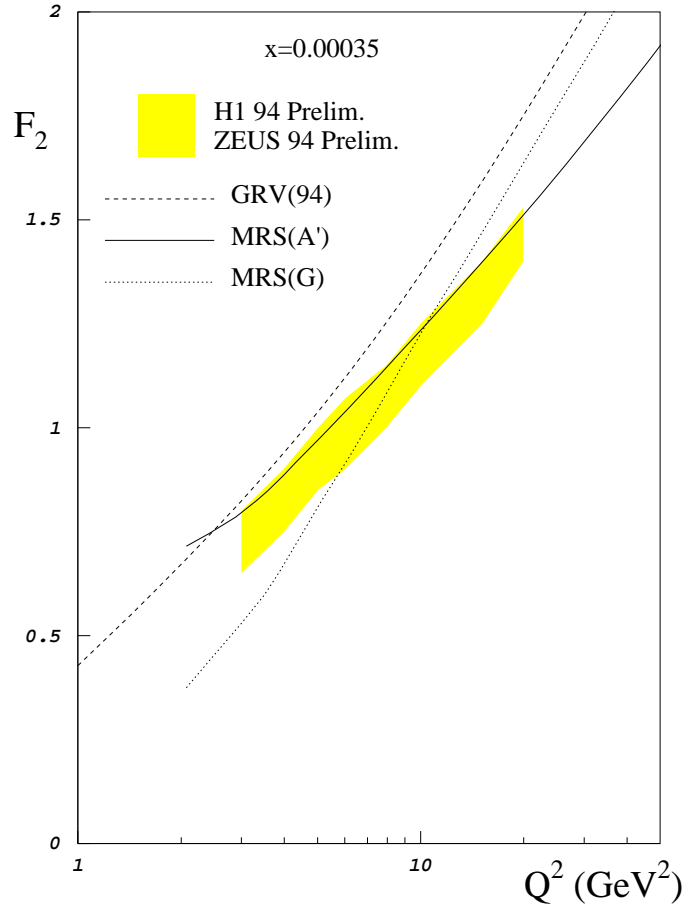


Figure 9: The values of  $F_2$  versus  $\ln Q^2$  at  $x = 3.5 \times 10^{-4}$  obtained from GRV [7] and MRS(A',G) [8] partons. The shaded band delimits the most recent measurements of the structure function obtained by the H1 and ZEUS collaborations [18].

We conclude that the HERA  $J/\psi$  photoproduction data offer a unique opportunity to distinguish between the various gluon distributions in a kinematic region ( $x = M_\psi^2/W^2 \simeq 10^{-3}$  and  $\overline{Q}^2 \simeq 2.5 \text{ GeV}^2$ ) where they are particularly distinct. In order to make a meaningful comparison we have computed several corrections to the lowest-order formula for the  $J/\psi$  cross section. The uncertainties are found to be greater in the predicted size of the cross section than in the  $W$  or, equivalently, the  $x$  dependence. That is the shape, rather than the normalisation, is the better discriminator between the various gluons. The comparison of the  $J/\psi$  cross section data with the values calculated using the gluons of three of the latest parton



sets was shown in Fig. 8. The shape (and the normalisation) predicted by the MRS(A') gluon is, within the theoretical accuracy, in excellent agreement with the measured values of the  $J/\psi$  photoproduction cross section. In fact the data appear to favour the MRS(A') gluon over the GRV gluon, and to rule out that of MRS(G).

A similar preference for the MRS(A') gluon is found by inspecting the slope of the most recent HERA measurements of the structure function  $F_2$  as a function of  $\ln Q^2$  as shown, for example, in Fig. 9. This slope is an independent measure of the gluon at small  $x$ , though, as anticipated, it is not such a sensitive probe as the  $W$  dependence of the HERA diffractive  $J/\psi$  cross section data. However, if combined together, the HERA measurements of the diffractive cross section  $\sigma(\gamma p \rightarrow J/\psi p)$  and of the slope  $\partial F_2 / \partial \ln Q^2$  offer an excellent opportunity to pin down the gluon density for  $x \lesssim 10^{-3}$ .

## Acknowledgements

We thank Drs. R. C. E. Devenish and M. R. Whalley for organizing the Durham Workshop on ‘‘HERA Physics’’, where this work originated. We thank the UK Particle Physics and Astronomy Research Council and the Royal Society for financial support. Also EML thanks CNPq of Brazil for financial support.

## References

- [1] M. G. Ryskin, Z. Phys., **C37** (1993) 89.
- [2] S. J. Brodsky et al., Phys. Rev., **D50** (1994) 3134.
- [3] Z. Chan, private communication to A. H. Mueller.
- [4] A. Donnachie and P. Landshoff, Phys. Lett. **B185** (1987) 403; Nucl. Phys. **B311** (1989) 509;  
J. R. Cudell, Nucl. Phys. **B336** (1990) 1.
- [5] ZEUS collaboration: M. Derrick et al., Phys. Lett. **B350** (1995) 120;  
ZEUS and H1 collaborations: preliminary ‘94 data presented at the Durham Workshop on HERA Physics, Sept. 1995, to be published.
- [6] E401 collaboration: M. Binkley et al., Phys. Rev. Lett., **48** (1982) 73;  
E561 collaboration: B. H. Denby et al., Phys. Rev. Lett., **52** (1984) 795.
- [7] M. Glück, E. Reya and A. Vogt, Z. Phys., **C67** (1995) 433.
- [8] A. D. Martin, R. G. Roberts and W. J. Stirling, Phys. Lett., **B354** (1995) 155.
- [9] L. V. Gribov, E. M. Levin and M. G. Ryskin, Phys. Rep., **100** (1983) 1.

- [10] A. A. Anselm and V. N. Gribov, Phys. Lett. **B40** (1972) 487.
- [11] L. Frankfurt, W. Koepf and M. Strikman, Tel-Aviv University preprint, TAUP-2290-95.
- [12] E.M. Levin, A.D. Martin, R.G. Roberts and M.G. Ryskin, in preparation.
- [13] C. Quigg and J. L. Rosner, Phys. Lett., **71B** (1977) 153;  
E. Eichten et al., Phys. Rev., **D17** (1978) 3090.
- [14] A. El-Khadra, G. Hockney, A. S. Kronfeld and P. B. Mackenzie, Phys. Rev. Lett., **69** (1992) 729.
- [15] H. Jung, D. Krücker, C. Greub and D. Wyler, Z. Phys. **C60** (1993) 721.
- [16] E. Gotsman, E. M. Levin and U. Maor, Tel-Aviv University preprint TAUP-2283-95.
- [17] M. Kramär, J. Zunft, J. Steegborn and P. M. Zerwas, Phys. Lett., **B348** (1995) 657.
- [18] H1, ZEUS preliminary data presented at the Durham Workshop on HERA Physics, Sept. 1995, to be published.